Advances in Radiation Oncology (2021) 6, 100745

advances in radiation oncology

www.advancesradonc.org

Scientific Article

Implementation of a Knowledge-Based Treatment Planning Model for Cardiac-Sparing Lung Radiation Therapy

Joseph Harms, PhD,[a,b,*] Jiahan Zhang, PhD,[a] Oluwatosin Kayode, MS,[a] Jonathan Wolf, MS,[a] Sibo Tian, MD,[a] Neal McCall, MD,[a] Kristin A. Higgins, MD,[a] Richard Castillo, PhD,[a] and Xiaofeng Yang, PhD[a]

[a]*Department of Radiation Oncology and Winship Cancer Institute, Emory University, Atlanta, Georgia;* [b]*Department of Radiation Oncology, University of Alabama at Birmingham, Birmingham, Alabama*

Received March 26, 2021; revised June 1, 2021; accepted June 11, 2021

Abstract

Purpose: High radiation doses to the heart have been correlated with poor overall survival in patients receiving radiation therapy for stage III non-small cell lung cancer (NSCLC). We built a knowledge-based planning (KBP) tool to limit the dose to the heart during creation of volumetric modulated arc therapy (VMAT) treatment plans for patients being treated to 60 Gy in 30 fractions for stage III NSCLC.

Methods and Materials: A previous study at our institution retrospectively delineated intracardiac volumes and optimized VMAT treatment plans to reduce dose to these substructures and to the whole heart. Two RapidPlan (RP) KBP models were built from this cohort, 1 model using the clinical plans and a separate model using the cardiac-optimized plans. Using target volumes and 6 organs at risk (OARs), models were trained to generate treatment plans in a semiautomated process. The cardiac-sparing KBP model was tested in the same cohort used for training, and both models were tested on an external validation cohort of 30 patients.

Results: Both RP models produced clinically acceptable plans in terms of target coverage, dose uniformity, and dose to OARs. Compared with the previously created cardiac-optimized plans, cardiac-sparing RPs showed significant reductions in the mean dose to the esophagus and lungs while performing similarly or better in all evaluated heart dose metrics. When comparing the 2 models, the cardiac-sparing RP showed reduced ($P < .05$) heart mean and maximum doses as well as volumes receiving 60 Gy, 50 Gy, and 30 Gy.

Conclusions: By using a set of cardiac-optimized treatment plans for training, the proposed KBP model provided a means to reduce the dose to the heart and its substructures without the need to explicitly delineate cardiac substructures. This tool may offer reduced planning time and improved plan quality and might be used to improve patient outcomes.

Introduction

Radiation therapy to the thorax is correlated with cardiovascular toxicity in patients treated for lymphoma,[1] breast cancer,[2] esophageal cancer,[3] and lung cancer.[4,5] Although radiation-induced congestive heart failure or

Sources of support: This work had no specific funding.

Disclosure: Dr Higgins reports receiving grants from RefleXion and personal fees from AstraZeneca, Genetech, Presica, and Varian outside the submitted work.

*Corresponding author: Joseph Harms, PhD; E-mail: jharms@uabmc.edu

https://doi.org/10.1016/j.adro.2021.100745

myocardial infarction can take years to manifest,[6,7] acute toxicities, such as pericarditis, have also been found among patients receiving high cardiac doses.[8] In the NRG Oncology Radiation Therapy Oncology Group radiation dose escalation trial (RTOG 0617), increased cardiac dose was associated with poorer survival outcomes in the high-dose arm of the study.[9] Specifically, the cardiac volumes receiving 5 Gy and 30 Gy (V5 and V30, respectively) were associated with higher death rates. Other studies have shown that an increased maximum dose to the heart correlates with higher death rates as soon as 6 months after treatment.[10,11] There has been a recent focus on investigating the radiation dose to specific cardiac substructures.[12-14] McWilliam et al found that the maximum dose to a cardiac region consisting of the right atrium, right coronary artery, and ascending aorta had the greatest effect on survival compared with the mean and maximum dose to the whole heart as well as other regions of the heart.[15] In a preclinical murine model study, Ghita et al found that the base of the heart was more radiosensitive than the middle or apex and that whole-heart dosimetric parameters did not predict physiological changes from irradiation of subvolumes of the heart.[16]

When cardiac substructures are contoured at the treatment planning stage, radiation treatment plans can be designed to limit the dose to these structures.[17] However, the task of delineating cardiac substructures can be time consuming, and it is not typically clinically feasible to optimize treatment plans to limit the dose to cardiac substructures. Another way to translate substructure dose reduction to all cases is to use knowledge-based planning (KBP) to incorporate geometric and dose information from a set of treatment plans to induce the optimization process for new cases. KBP can be used to estimate 3-dimensional dose distributions or dose-volume histograms (DVHs).[18] KBP has been widely implemented across many different disease sites and allows for a means of partially automating the treatment planning process and reducing variability in plan quality.[19] In the setting of lung irradiation, KBP studies have shown improvements in V5, V20, and mean lung dose.[20] Other KBP models have been used to incorporate more information to the treatment planning process, such as training a model with functional lung volumes to allow for more patient-specific optimization.[21] Similar to a study by Faught et al,[21] in which the authors used a set of highly curated plans with lung functional avoidance to build a model, in this study, we trained a KBP model for thoracic irradiation using a subset of treatment plans that were optimized to reduce the dose to the heart and substructures of the heart. The purpose of this study was to determine whether using a KBP model trained with cardiac-sparing lung radiation therapy plans can reduce cardiac dose without compromising target coverage or increasing doses to other organs at risk (OARs). Furthermore, using a subset of validation cases, we tested the model's ability to reduce the dose to cardiac substructures in a separate patient cohort without substructure delineation.

Methods

To generate plans for model input, clinical treatment plan data were retrospectively collected for 31 patients treated to a standard regimen of 60 Gy in 30 fractions for stage III non-small cell lung cancer (NSCLC) at our institution. Approval for this retrospective study was obtained by the internal review board of Emory University. This cohort of patients all had 2 pre-existing treatment plans. The first group of plans were the clinically used plans, which were planned by our dosimetry team and approved by the treating radiation oncologist. In addition to the clinical plans, our dosimetry team retrospectively generated a cardiac-optimized plan for each patient. To generate the cardiac-optimized plans, 15 cardiac substructures were delineated on free-breathing computed tomography (CT) scans acquired at the time of CT simulation. Substructures delineated were the left and right atria and ventricles, the coronary arteries (left anterior descending, left circumflex, left main, and right coronary artery), the ascending aorta, the pulmonary artery, the superior vena cava, and the valves of the heart (atrial, mitral, pulmonary, and tricuspid).

Contours were transferred via rigid registration to the averaged 4-dimensional computed tomography for dose calculation. Volumetric modulated arc therapy (VMAT) treatment plans using 2 to 3 arcs were optimized to meet clinical DVH constraints for the heart, lungs, esophagus, and spinal cord. In addition, in the reoptimized cardiac-sparing plans, the dose to cardiac substructures was reduced according to as low as reasonably achievable (ALARA) principles. This article discusses differences between the clinical plans and the cardiac-optimized plans in detail, and full dosimetric comparisons have been previously reported.[17]

RapidPlan (RP) is a model-based KBP module integrated within the Eclipse treatment planning system (Varian Medical Systems, Palo Alto, California). It extracts treatment planning knowledge embedded in prior treatment plans by establishing correlations between plan DVHs and patient anatomy and beam geometry features.[22] Once trained, an RP model can generate OAR DVH estimates for a future patient based on structure contours and beam placements. During training, input structures are decomposed into 4 functional subregions (out-of-field, mutli-leaf collimator transmission, overlap, and in-field) which are modeled separately to reproduce input DVHs. A means-and-standard-deviation model is used for low-dose modeling in the out-of-field and mutli-leaf collimator transmission regions. The overlap subregion contains voxels that lie in both the target organ and an OAR. These voxels are assumed to receive the full prescription dose. The in-field subregion contains voxels

that lie in the beam's-eye view but not within the target volume, and this portion of the DVH is modeled by applying principal component analysis to the known in-field DVH and a geometry-based expected dose (GED) histogram, which is analogous to a distance between a voxel and the target volume. Stepwise multiple regression is used to fit principal component scores of the DVH to a set of anatomic features, including GED principal scores, planning target volume (PTV), OAR volume, OAR and PTV overlap, and the percentage of the OAR that is outside the treatment fields. For a new patient, DVHs of the 4 subregions are estimated and combined to form the whole OAR DVH. In addition to producing DVH estimates, RP allows users to define optimization templates with constraints based on DVH predictions.

Two models were trained for this study. The proposed cardiac-sparing model used the cardiac-optimized treatment plans as input. Input structures were the clinical target volume (CTV), PTV, and 8 OAR structures: heart, lungs (ipsilateral, contralateral, whole lungs, and lungs cropped out of the CTV), esophagus, spinal cord, and a spinal cord planning-risk volume (PRV) based on a 5-mm expansion. In addition to the line constraints generated by RP for optimization, specific DVH dose constraints were added to the optimization template to meet certain standard clinical metrics, such as the volume of lungs receiving 20 Gy (V20). The full optimization template can be found in Table S1.

RapidPlan was used to retrospectively replan cases for the 31 patients used to build the model, comparing model inputs directly to model outputs. We refer to this set of plans as the training cohort. When using RP to generate models, optimization objectives were not modified in any way as optimization progressed. The RP-generated plans were compared only with the cardiac-sparing VMAT plans because a previous study showed that these plans improved dose metrics, compared with the clinical plans, for all thoracic OARs in addition to the heart.[17] Beam parameters such as arc length, collimator angle, and energy were held constant between all initial plans and replans. Patients were treated on either Varian Trilogy or TrueBeam (Varian Medical Systems, Palo Alto, CA) with 6 MV beams.

The cardiac-sparing RP model was then used to retrospectively generate plans in a separate cohort of 30 patients treated for stage III NSCLC (the validation cohort), and they were all treated to 60 Gy in 30 fractions and had target volumes near or overlapping the heart. The PTV sizes were similar between the 2 groups, with means (SDs) of 442.5 (254.5) cm^3 in the training cohort and 460.2 (246.7) cm^3 in the validation cohort.

To further test the cardiac-sparing model, a second independent RP model was trained using the clinical plans from the training cohort, which we called the clinical RP model. The same optimization objective template was paired with DVH estimates from this model, and plans were regenerated for the validation cohort. This allowed us to evaluate whether changes in plan quality were owed to the input data to the cardiac-optimized RP model or the optimization objective template used alongside the DVH estimates. As an example of the difference in model inputs, Figure S1 shows the mean input heart DVH for both models. Further dosimetric differences between the input plan models can be seen in Table S2.

To investigate dose changes to the cardiac substructures in addition to the whole heart for the validation cohort, we retrospectively delineated the cardiac substructures of 22 patients. The maximum and mean doses to these structures were evaluated for the original plan, the clinical RP, and the cardiac-sparing RP.

Paired, 2-tailed t tests were applied to resulting DVH metrics, comparing the cardiac-sparing RP first with the clinical plans and then with the clinical RP. Statistical significance was set at $P < .05$. All dose calculations were carried out in Eclipse using the Anisotropic Analytical Algorithm, version 15.6.05. When generating plans with the RP models, optimization was initialized using the DVH estimation tool and then proceeded without intervention. Arc parameters, including numbers of arcs and control points, were held constant when replanning using RP. For the final evaluation, all plans were normalized so that prescription dose covered 95% of the PTV.

Results

Training cohort

Dose distributions from 5 patients in the training cohort are shown in Figure 1. These patients were chosen to show how the RP model performed on the most challenging cases in the data set. Quantitative results for all patients in the training cohort are summarized in Table 1. As shown in Figure 1, the RP model produced plans with dose distributions similar to those of the model input plans. There were significant reductions in the volume of the heart receiving the prescription dose, in the mean lung dose, and in the V20 in the lungs (Table 1). The only dose evaluation metric in which the RP was significantly inferior to the input plans was in the maximum dose to the PTV; however, the PTV minimum dose was significantly improved.

Validation cohort

Dose distributions from 5 patients in the validation cohort are shown in Figure 2. Both the clinical and cardiac-sparing RP models produced more conformal plans, and both allowed for cardiac sparing. Mean quantitative results from all patients in the validation cohort are

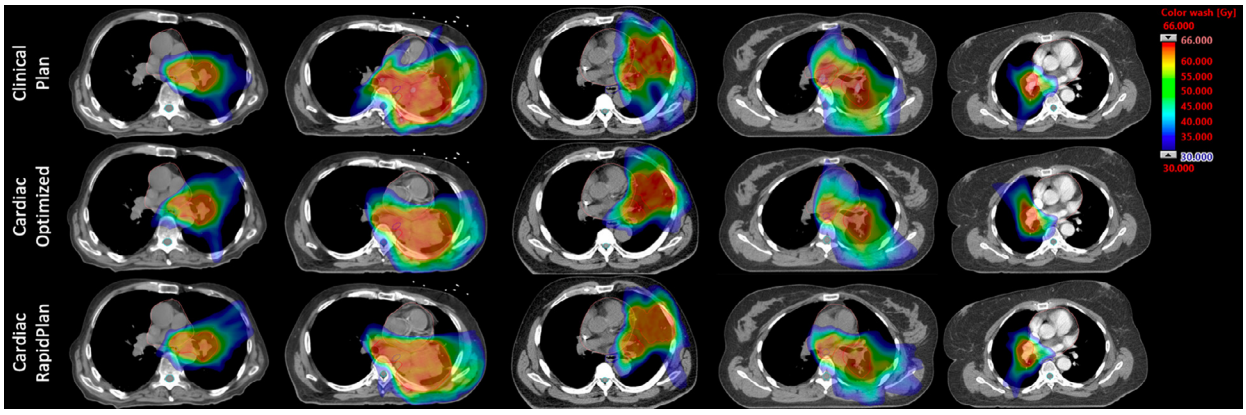

Fig. 1 Dose distributions from 5 patients with the highest mean heart dose from the training cohort. The clinical plans were the original plans for treatment, the cardiac optimized plans were the RapidPlan (RP) model input, and the cardiac-sparing RPs were generated using the model proposed in this study. Each column shows 3 plans from 1 patient, and all images correspond to the same computed tomography scan slice. The planning target volume is shown in red, the heart in pink, the spinal cord in cyan, and the esophagus in blue. The dose color wash ranges from 30 Gy (blue) to 66 Gy (red).

shown in Table 2. Although both RP models showed improvements over the clinical plan, the cardiac-sparing model showed statistically significant improvement over the clinical model in all evaluated heart metrics except V5. However, this came with a tradeoff because the clinical RP model had significant improvements in the mean dose to the esophagus and the mean dose and V20 for the lungs. Both models performed similarly in PTV coverage.

Both RP models improved on the clinical plans at all dose levels in the heart and for doses less than 35 Gy in the lungs (Fig 3). The cardiac-sparing RP showed a lower mean cardiac DVH than the clinical RP at all dose levels between 0 and 66 Gy, with the largest benefit being in the 10 to 25 Gy range. Although both models produced smaller low-dose volumes in the lungs, the clinical plans reduced volumes receiving doses greater than 45 Gy. In addition, Figure 3 (inset d) shows that although the clinical RP and cardiac-sparing RPs performed similarly in the lungs, the clinical RP mean DVH was lower by almost 0.5%, with the largest differences between the 20 and 40 Gy levels.

Substructure validation

A secondary endpoint of this study was to encode the information provided by the substructure contours and

Table 1 Selected DVH metrics for the PTV and OARs for patients in the training cohort*

Structure	Metric	Cardiac-sparing RP	Cardiac-optimized plan	*P* value
PTV	Maximum, Gy	67.88 ± 1.20	66.62 ± 1.21†	<.001
	Minimum, Gy	51.92 ± 4.13†	50.66 ± 3.64	.02
	D2, Gy	64.85 ± 1.77	64.68 ± 0.98	.55
	D98, Gy	59.10 ± 0.38	58.83 ± 0.66	.07
Esophagus	Mean, Gy	18.56 ± 5.37†	20.02 ± 6.31	<.001
Heart	Maximum, Gy	62.68 ± 6.70†	63.74 ± 6.78	.004
	Mean, Gy	10.58 ± 5.65	10.60 ± 6.43	.95
	V60, %	2.15 ± 2.53†	2.39 ± 2.81	.02
	V50, %	4.20 ± 4.04	4.24 ± 4.21	.73
	V30, %	9.08 ± 7.05	9.66 ± 8.88	.35
	V5, %	49.59 ± 26.43	48.83 ± 27.33	.46
Lungs	Mean, Gy	13.16 ± 2.21†	13.87 ± 2.36	<.001
	V20, %	21.67 ± 4.48†	23.40 ± 4.95	<.001
	V5, %	56.59 ± 10.22	56.45 ± 8.03	.89
Spinal cord	Maximum, Gy	30.23 ± 3.37	28.62 ± 7.56	.14

Abbreviations: D2 and D98 = doses to 2% and 98% of the volumes, respectively; DVH = dose-volume histogram; OAR = organ at risk; PTV = planning target volume; RP = RapidPlan; V5, V30, V50, and V60 = the cardiac volumes receiving 5, 30, 50, and 60 Gy, respectively.

* Means and standard deviations are shown from the 31 plans from the patient cohort.

† Statistically significantly improved performance with the cardiac-sparing RP model ($P < .05$).

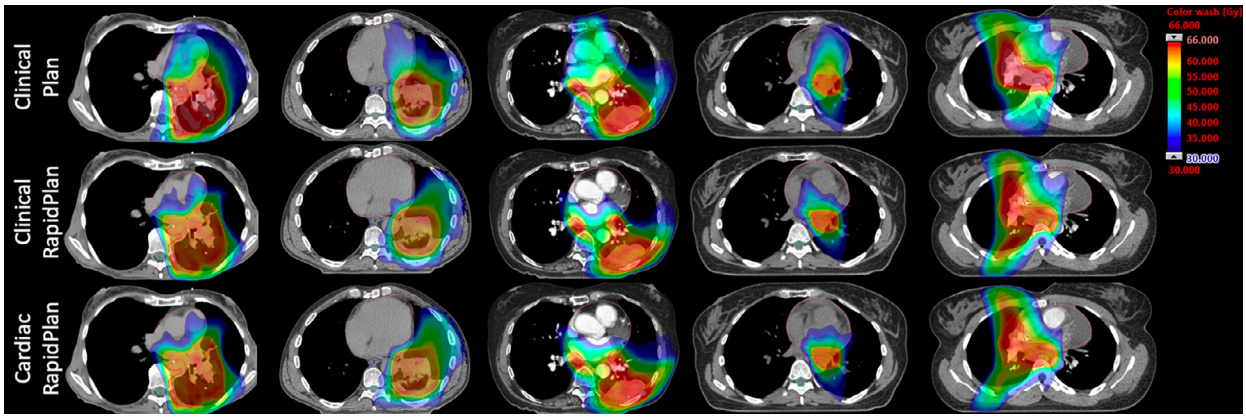

Fig. 2 Dose distributions from 5 patients with the highest mean heart dose from the validation cohort. The first row shows the dose from the plans that were used for treatment, the second row shows the dose from plans generated with the clinical RapidPlan (RP) model, and the third row shows the dose from plans generated with the cardiac-sparing RP model. Each column shows the 3 plans from 1 patient, and all images correspond to the same computed tomography scan slice. The planning target volume is shown in red, the heart in pink, the spinal cord in cyan, and the esophagus in blue. The dose color wash ranges from 30 Gy (blue) to 66 Gy (red).

subsequent optimization of the cardiac-sparing plans into the RP model. The resulting mean and maximum doses for cardiac substructures grouped by type, evaluated in 22 patients from the validation cohort, are shown in Table 3. Individual substructure dose metrics are shown in Table E3. Whereas the cardiac-sparing RP did not statistically significantly outperform the clinical RP in all metrics, it produced lower maximum doses for all grouped substructures within the heart (chambers, coronary arteries, and valves).

Discussion

Radiation-induced heart disease is a posttreatment toxicity that needs further study; however, some literature has supported the hypothesis that the incidence of radiation-induced heart disease increases with radiation dose, possibly with no threshold.[2,23] In addition to influencing posttreatment toxicities, the radiation dose to the heart can lead to decreased patient activity levels during the course of radiation therapy.[24] Although recent studies

Table 2 Selected DVH metrics from the validation cohort*

Structure	Metric	Cardiac-sparing RP	Clinical plan	*P* value	Clinical RP	*P* value†
PTV	Maximum, Gy	68.01 ± 1.52	67.51 ± 2.43	.23	68.09 ± 1.42	.48
	Minimum, Gy	51.48 ± 4.07	5.46 ± 4.62	.26	51.13 ± 4.20	.07
	D2, Gy	64.38 ± 1.09‡	65.49 ± 1.97	<.001	64.52 ± 1.11	.01
	D98, Gy	59.17 ± .37	58.99 ± .39	.006	59.17 ± .36	.90
Esophagus	Mean, Gy	19.57 ± 8.10	22.68 ± 8.62	<.001	19.17 ± 7.88	.003
Heart	Maximum, Gy	56.77 ± 16.23‡	58.54 ± 16.09	.02	57.29 ± 15.63	.03
	Mean, Gy	8.03 ± 6.16‡	9.79 ± 7.96	<.001	8.48 ± 6.48	<.001
	V60, %	.80 ± 1.06	1.34 ± 1.39	<.001	.85 ± 1.10	.05
	V50, %	2.47 ± 2.20‡	3.32 ± 3.23	.01	2.58 ± 2.32	.001
	V30, %	6.99 ± 8.27‡	1.74 ± 12.67	.004	8.02 ± 8.88	.002
	V5, %	39.48 ± 29.28	42.64 ± 3.51	<.001	39.74 ± 28.90	.40
Lungs-CTV	Mean (Gy)	13.47 ± 3.57	13.93 ± 3.17	.006	13.38 ± 3.56	.001
	V20, %	22.85 ± 6.54	23.99 ± 6.09	.008	22.67 ± 6.55	.05
	V5, %	59.25 ± 15.08	6.61 ± 13.18	.29	59.14 ± 15.15	.53
Spinal cord	Max (Gy)	29.95 ± 3.84	29.64 ± 9.43	.82	3.01 ± 3.75	.67

Abbreviations: CTV = clinical target volume; DVH = dose-volume histogram; PTV = planning target volume; RP = RapidPlan; V5, V20, V30, V50, and V60 = the cardiac volumes receiving 5, 20, 30, 50, and 60 Gy, respectively.

* Means and standard deviations are shown from the 30 plans from the validation cohort.

† All *P* values are for comparisons with the cardiac-sparing RP.

‡ Statistically significant difference between the cardiac-sparing RP and both comparison plans.

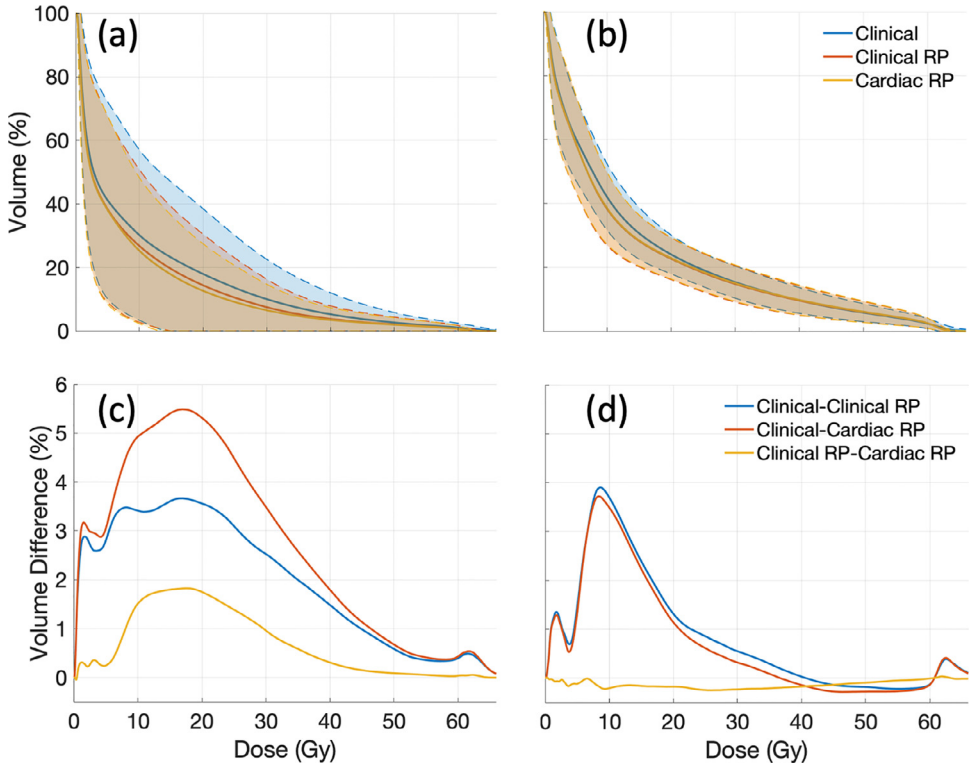

Fig. 3 Mean dose volume histograms (DVHs) for (A) heart and (B) lung for all patients in the validation cohort, with shaded regions showing 1 standard deviation for each data set. (C, D) The insets show differences in the DVHs between all 3 plan types.

have shown correlation between cardiac toxicities and dose to specific cardiac substructures,[15,25] a full understanding of the relationship between dose to these substructures and specific toxicities is lacking. Given this lack of data for toxicity analysis for cardiac substructures, it is reasonable to follow ALARA principles when creating radiation therapy treatment plans when the heart is in the radiation field, especially because survival among patients with stage III NSCLC continues to increase.[26]

One advantage of the proposed method is the ability to spare cardiac substructures without the need for substructure contours. Although improvements over the clinical RP were not all statistically significant (Table 3), the improvements from the clinical plans to the cardiac-sparing RP were substantial (reductions in mean dose of 1.4 Gy, 3.3 Gy, and 3.0 Gy to the chambers, coronary arteries, and valves, respectively). On average, it can take 1 to 2 hours to delineate cardiac substructures, and optimization using these substructures can add up to an hour to the treatment planning process. By implementing the proposed method, we were able to save these 2 to 3 hours per

Table 3 Maximum and mean doses in Gy for all cardiac substructures*

Structure	Metric	Cardiac-sparing RP	Clinical plan	*P* value†	Clinical RP	*P* value†
Chambers	Maximum	27.70 ± 23.36‡	3.14 ± 23.93	<.001	28.33 ± 23.58	.004
	Mean	7.31 ± 9.66‡	8.56 ± 1.94	<.001	7.56 ± 9.91	.002
Coronary arteries	Maximum	19.39 ± 18.85‡	22.72 ± 2.31	<.001	2.76 ± 19.31	<.001
	Mean	11.81 ± 13.33‡	14.30 ± 15.60	<.001	12.32 ± 13.55	.01
Valves	Maximum	12.50 ± 14.77‡	15.46 ± 18.40	<.001	13.22 ± 15.63	.01
	Mean	8.17 ± 9.99	1.61 ± 13.34	<.001	8.50 ± 1.37	.08
Great vessels	Maximum	62.93 ± 6.61	63.51 ± 6.76	.02	62.88 ± 6.48	.73
	Mean	34.08 ± 13.67	36.17 ± 13.98	<.001	34.29 ± 13.79	.15

Abbreviation: RP = RapidPlan.

* Means and standard deviations were calculated from the 22 patient data sets in the validation cohort with cardiac substructure contours.

† All *P* values are for comparisons with the cardiac-sparing RP.

‡ Statistically significant difference between the cardiac-sparing RP and both comparison plans.

plan and maintain plan quality while seeing a reduction in cardiac and substructure doses.

The RP approach allows for hands-free optimization; however, it does have some limitations. Because the optimization is not actively monitored, there are certain OARs that are not pushed to the lowest dose possible. For example, the maximum dose to the spinal cord was close to 30 Gy for all RPs, even though it may have been pushed to less than 20 Gy in the original clinical plans. This may also be owed to RP's approach to DVH estimation, which relies on principal component analysis. Because the maximum dose is typically the only metric of interest for the spinal cord, treatment planners typically restrict the maximum dose and do not limit the entire DVH curve. Therefore, larger variability is expected in spinal cord DVHs. As a result, spinal cord predictions likely were not as accurate as those for other organs, and when the prediction is higher, the final dose will be higher.

Some tradeoff is necessary to achieve the cardiac sparing shown in this study. In the validation study, the clinical RP model significantly outperformed the cardiac-sparing RP model in the esophagus mean dose, lung mean dose, and lung V20. The dosimetric improvements for both RP models also came at the cost of an increase in monitor units (MU): 489 $\pm$ 78 for the original versus 566 $\pm$79 for the cardiac-sparing RP ($P < .001$) and 569 $\pm$ 76 for the clinical RP ($P < .001$). This finding is consistent with that of Tahmbe et al, who found that for their lung KBP model, reoptimized plans statistically significantly increased plan complexity in both MU and MU/degree.[20] Tahmbe et al further found that this increased complexity did not affect plan deliverability.

A limitation of the current study's design is that all plans used for model training were developed as part of a previous retrospective study. A single observer delineated all thoracic OARs, and 2 dosimetrists generated all treatment plans with a specific list of optimization goals. All plans were generated within 1 institution, and the sample size is small. Further validation using multi-institutional prospective data are necessary to validate the findings of this model and to account for differences between planners.

The nature of the model input plans also means that the input data set for model training can be expected to show less variation than a standard clinical data set. Although the sample size for this study was small, Fogliata et al previously suggested that an RP model for thoracic radiation therapy could be adequately trained with 27 patients, similar to the 31 used in this study.[27] Fogliata et al found that for the heart DVH, more than 99% of cases in their study were reproduced in the DVH or GED components with an average reduced χ^2 value of 1.20. DVH modeling of the heart in the current study's proposed model also produced a reduced χ^2 of 1.20.

Conclusions

The KBP model proposed in this study was applied to patients receiving 60 Gy in 2-Gy fractions for stage III NSCLC. The model preserved the cardiac sparing that was shown in a previous study[17] without the need for contouring intracardiac structures. The proposed model may allow for reduction in the cardiac dose without compromising target coverage or increasing the dose to other thoracic OARs. In addition, the model was able to capture dosimetric information about cardiac substructures, which allowed for a decreased dose to these substructures even if they were not delineated as part of the treatment planning process. Use of this model may allow for semiautomated treatment planning in a cohort of patients who are typically difficult to plan, and the reduction in heart dose achieved by the model in this study could potentially limit future toxicities.

Supplementary materials

Supplementary material associated with this article can be found, in the online version, at doi:10.1016/j.adro.2021.100745.

References

1. Ng AK. Review of the cardiac long-term effects of therapy for Hodgkin lymphoma. *Br J Haematol*. 2011;154:23–31.
2. Darby SC, Ewertz M, McGale P, et al. Risk of ischemic heart disease in women after radiotherapy for breast cancer. *N Engl J Med*. 2013;368:987–998.
3. Beukema JC, van Luijk P, Widder J, Langendijk JA, Muijs CT. Is cardiac toxicity a relevant issue in the radiation treatment of esophageal cancer? *Radiother Oncol*. 2015;114:85–90.
4. Douillard J-Y, Rosell R, De Lena M, Riggi M, Hurteloup P, Mahe M-A. Impact of postoperative radiation therapy on survival in patients with complete resection and stage I, II, or IIIA non−small-cell lung cancer treated with adjuvant chemotherapy: The Adjuvant Navelbine International Trialist Association (ANITA) randomized trial. *Int J Radiat Oncol Biol Phys*. 2008;72:695–701.
5. Ferris MJ, Jiang R, Behera M, Ramalingam SS, Curran WJ, Higgins KA. Radiation therapy is associated with an increased incidence of cardiac events in patients with small cell lung cancer. *Int J Radiat Oncol Biol Phys*. 2018;102:383–390.
6. Darby SC, McGale P, Taylor CW, Peto R. Long-term mortality from heart disease and lung cancer after radiotherapy for early breast cancer: Prospective cohort study of about 300 000 women in US SEER cancer registries. *Lancet Oncol*. 2005;6:557–565.
7. van Nimwegen FA, Schaapveld M, Janus CPM, et al. Cardiovascular disease after Hodgkin lymphoma treatment: 40-Year disease risk. *JAMA Intern Med*. 2015;175:1007–1017.
8. Darby SC, Cutter DJ, Boerma M, et al. Radiation-related heart disease: Current knowledge and future prospects. *Int J Radiat Oncol Biol Phys*. 2010;76:656–665.
9. Bradley JD, Paulus R, Komaki R, et al. Standard-dose versus high-dose conformal radiotherapy with concurrent and consolidation carboplatin plus paclitaxel with or without cetuximab for patients with stage IIIA or IIIB non-small-cell lung cancer (RTOG 0617): A

randomised, two-by-two factorial phase 3 study. *Lancet Oncol*. 2015;16:187–199.
10. Vivekanandan S, Landau DB, Counsell N, et al. The impact of cardiac radiation dosimetry on survival after radiation therapy for non-small cell lung cancer. *Int J Radiat Oncol Biol Phys*. 2017;99:51–60.
11. Haq R, Hotca A, Apte A, Rimner A, Deasy JO, Thor M. Cardio-pulmonary substructure segmentation of radiotherapy computed tomography images using convolutional neural networks for clinical outcomes analysis. *Phys Imag Radiat Oncol*. 2020;14:61–66.
12. van den Bogaard VAB, Ta BDP, van der Schaaf A, et al. Validation and modification of a prediction model for acute cardiac events in patients with breast cancer treated with radiotherapy based on three-dimensional dose distributions to cardiac substructures. *J Clin Oncol*. 2017;35:1171–1178.
13. Patel SA, Mahmood S, Nguyen T, et al. Comparing whole heart versus coronary artery dosimetry in predicting the risk of cardiac toxicity following breast radiation therapy. *Int J Radiat Oncol Biol Phys*. 2018;102(3, Suppl):S46.
14. Abouegylah M, Braunstein LZ, Alm El-Din MA, et al. Evaluation of radiation-induced cardiac toxicity in breast cancer patients treated with Trastuzumab-based chemotherapy. *Breast Cancer Res Treat*. 2019;174:179–185.
15. McWilliam A, Khalifa J, Vasquez Osorio E, et al. Novel methodology to investigate the impact of radiation dose to heart sub-structures on overall survival. *Int J Radiat Oncol Biol Phys*. 2020;108:1073–1081.
16. Ghita M, Gill EK, Walls GM, et al. Cardiac sub-volume targeting demonstrates regional radiosensitivity in the mouse heart. *Radiother Oncol*. 2020;152:216–221.
17. Ferris M, Martin K, Switchenko J, et al. Sparing cardiac substructures with optimized volumetric arc therapy and intensity modulated proton therapy in thoracic radiation for locally advanced non-small cell lung cancer. *Pract Radiat Oncol*. 2019;9:473–481.
18. Ge Y, Wu QJ. Knowledge-based planning for intensity-modulated radiation therapy: A review of data-driven approaches. *Med Phys*. 2019;46:2760–2775.
19. Moore KL, Appenzoller LM, Tan J, Michalski JM, Thorstad WL, Mutic S. Clinical implementation of dose-volume histogram predictions for organs-at-risk in IMRT planning. *J Phys Conf Ser*. 2014;489: 012055.
20. Tambe NS, Pires IM, Moore C, Cawthorne C, Beavis AW. Validation of in-house knowledge-based planning model for advance-stage lung cancer patients treated using VMAT radiotherapy. *Br J Radiol*. 2020;93: 20190535.
21. Faught AM, Olsen L, Schubert L, et al. Functional-guided radiotherapy using knowledge-based planning. *Radiother Oncol*. 2018;129:494–498.
22. Systems VM. *Elcipse Photon and Electron Algorithms Reference Guide*. Varian Medical Systems, Inc; 2018. Vol P1020505-003-C.
23. Wang K, Eblan MJ, Deal AM, et al. Cardiac toxicity after radiotherapy for stage III non-small-cell lung cancer: Pooled analysis of dose-escalation trials delivering 70 to 90 Gy. *J Clin Oncol*. 2017;35:1387–1394.
24. Paul S, Bodner WR, Garg M, Tang J, Ohri N. Cardiac irradiation predicts activity decline in patients receiving concurrent chemoradiation for locally advanced lung cancer. *Int J Radiat Oncol Biol Phys*. 2020;108:597–601.
25. Atkins KM, Chaunzwa TL, Lamba N, et al. Association of left anterior descending coronary artery radiation dose with major adverse cardiac events and mortality in patients with non−small cell lung cancer. *JAMA Oncol*. 2021;7:206–219.
26. Faivre-Finn C, Vicente D, Kurata T, et al. LBA49 Durvalumab after chemoradiotherapy in stage III NSCLC: 4-year survival update from the phase III PACIFIC trial. *Ann Oncol*. 2020;31:S1178–S1179.
27. Fogliata A, Belosi F, Clivio A, et al. On the pre-clinical validation of a commercial model-based optimisation engine: Application to volumetric modulated arc therapy for patients with lung or prostate cancer. *Radiother Oncol*. 2014;113:385–391.